Magnetic Properties of Nitroxide Spin Probes: Reliable Account of Molecular Motions and Nonspecific Solvent Effects by Time-Dependent and Time-Independent Approaches

ARTICLE *in* THE JOURNAL OF PHYSICAL CHEMISTRY B · SEPTEMBER 2010

Impact Factor: 3.3 · DOI: 10.1021/jp102232c · Source: PubMed

Magnetic Properties of Nitroxide Spin Probes: Reliable Account of Molecular Motions and Nonspecific Solvent Effects by Time-Dependent and Time-Independent Approaches

Michele Pavone,[†] Malgorzata Biczysko,[†,‡] Nadia Rega,[†] and Vincenzo Barone*[,‡]

Department of Chemistry "P. Corradini", University of Napoli Federico II and CR-INSTM "Village", Complesso Universitario Monte Sant'Angelo, Via Cintia 80126, Napoli, Italy; and Scuola Normale Superiore di Pisa, and INFN Sezione di Pisa, Piazza dei Cavalieri 7, I-56126, Pisa, Italy

Received: March 11, 2010; Revised Manuscript Received: August 5, 2010

Application of a new integrated computational approach for two widely used nitroxide spin probes allows to show unequivocally that proper account of stereoelectronic, environmental, and dynamical effects leads to magnetic properties in quantitative agreement with experimental results without the need of any empirical parameter. Together with their specific interest, our results point out, in our opinion, the importance of developing and validating computational approaches able to switch on and off different effects, including environmental and dynamical ones, in order to evaluate their specific role in determining the overall experimental outcome.

Introduction

Prediction of molecular properties by computer simulations is playing an increasing role toward reliable interpretation of experimental results for a broad range of systems of current chemical interest. Aid of in silico tools is particularly important in the field of molecular spectroscopy where the analysis of complex experimental spectra is seldom straightforward due to subtle interplay of different effects with nonnegligible yet not additive roles.[1] However, the standard quantum-mechanical (QM) approach, routinely applied by nonspecialists, is still based on the description of the molecular system under investigation in the gas phase and at its equilibrium minimum-energy structure.[1] Of course, such a static picture could hardly be related to real-life experiments for complex systems, performed at finite temperature and/or in condensed phases. Therefore, direct and effective comparison between in silico and in vitro experiments requires a proper account of both dynamical (i.e., molecular vibrations) and environmental (at least solvent librations) effects.

In particular, intramolecular dynamics affects several spectroscopic properties[2] and should be taken into account in the calculation of all spectroscopic parameters and not only for IR and Raman. In the case of electronic transitions, the vibrations are responsible for the vibronic structure of UV−vis absorption, fluorescence emission, or electronic circular dichroism spectra via the Franck−Condon selection rules (direct effect).[3] On the other hand, the energies governing transitions of interest in magnetic resonance spectroscopy are much lower than vibrational quanta, so that the long-time dynamics of the molecule, e.g., diffusion and rotational motions, determines the spectral line shapes. However, also in this case the temperature has the nonnegligible effect of averaging out the magnetic parameters over the structural fluctuations of the molecule, i.e., the short-time dynamics due to molecular vibrations (indirect effect).[4]

In the framework of the Born−Oppenheimer approximation, once a reliable and correlation-consistent description of the electronic potential energy surface is obtained, the method of choice for computing molecular vibrations is based on the solution of the nuclear Schrodinger equation.[5] Semirigid molecules are well described in terms of an harmonic approximation possibly supplemented by anharmonic terms issuing from an accurate yet feasible second-order perturbation scheme.[6] Spectroscopic observables are then computed through vibrational averaging with respect to the molecular normal modes, with temperature tuning the population of each mode.[7] Such a time-independent approach is very accurate for semirigid systems because it accounts for the QM nature of nuclear motions.

An alternative approach is represented by the sampling of nuclear motions in the classical phase space via molecular dynamics (MD) techniques.[8] In this case, the property of interest is obtained by extracting a consistent set of configurations from the MD trajectories, and by averaging the molecular parameters computed on each of these frames. In order to explore thermal averaging effects on molecular systems in the electronic ground state, ab initio MD (AIMD) simulations can be effectively exploited within the Car−Parrinello[9] scheme where the forces governing nuclear dynamics are computed from first principles, within the framework of plane-waves density-functional theory (DFT).[10] More recently, extension of the Car−Parrinello method to the atom-centered density matrix propagation scheme has allowed for the use of Gaussian-type orbitals as basis set for expanding the electronic degrees of freedom. It should be stressed that the use of atom-centered orbitals is particularly well adapted to study localized spectroscopic phenomena, while other advantages are related to the easy implementation into many-layer QM/MM models and to the possibility of applying last generation density functionals showing correct short-range and asymptotic behavior for AIMD simulations.[11] From a practical point of view, it is also remarkable that time-dependent approaches allow the use of different levels of theory for the generation of trajectories and for the computation of spectroscopic observables on a subset of the sampled structures. In particular, much longer samplings of potential energy hypersurfaces (PES) can be obtained by MD simulations using reliable force fields based on molecular mechanics (MM).[8] In this respect, the development of properly tailored force-fields stands

* To whom correspondence should be addressed. E-mail: vincenzo.barone@sns.it.
[†] University of Napoli "Federico II" and CR-INSTM "Village".
[‡] Scuola Normale Superiore di Pisa and INFN, Sezione di Pisa.

10.1021/jp102232c
Published on Web 08/18/2010

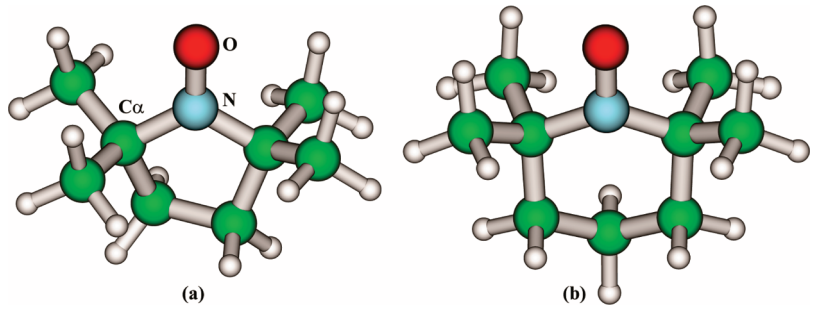

Figure 1. Structure and label of the Proxyl (a) and Tempo (b) spin-probe molecules.

as an important tool toward analysis of dynamic effects for larger molecular systems.[8b]

Time-independent and time-dependent approaches have been extensively exploited in the past decade for the prediction of molecular properties, from chemical reactivity to spectroscopy.[12] In fact, in several cases (like, e.g., simulations of optical spectra) the importance of vibrational effects is well recognized and has been accounted for following both routes.[1,3,12] Noteworthy are recent approaches based on the use of ab initio MD and correlation functions that allowed to address average dynamical effects on optical spectra by including also the relevant effects of fluctuations.[12b–f] Moreover, for very complex systems such as liquid solutions, the use of MD techniques becomes mandatory when specific solute−solvent interactions (e.g., hydrogen bonding in aqueous solutions) need to be properly averaged over solvent librations. Within this context, Car−Parrinello and hybrid QM/MM MD simulations provided very accurate results in the case of UV,[13] fluorescence,[14] NMR,[15] and ESR[16] spectroscopic properties, when combined to effective methods for the calculation of the molecular parameters of interest.

Despite these pioneering works, in our opinion, in the case of ESR spectroscopy widespread agreement on the proper treatment of short-time thermal fluctuations and, more importantly, about their effects on the computed parameters, is still lacking. For such reasons, the present contribution addresses the analysis of the subtle, but nonnegligible, indirect dynamic effects on ESR parameters (namely the nitrogen hyperfine coupling constant, hcc_N, and **g**-tensor isotropic shift, Δg_{iso}) by exploiting the above-mentioned time-independent and time-dependent routes. For a neat comparison, the same level of theory has been employed for both approaches, as well as for the calculation of magnetic parameters. In fact, the combination of QM computations of magnetic tensors in solution with the calculations of long-time diffusive motions within a stochastic Liouville equation approach could lead to an effective simulation of ESR spectra just starting from the chemical formula of the spin probe.[17] However, in the present contribution we prove that either the neglect or a poor description of molecular vibrations' effects could lead to qualitatively unreliable values of magnetic tensors, jeopardizing any further predictions based on these quantities.

Moreover, despite the methodological focus of the present work, our test cases do not correspond to toy models, but to two real-size nitroxide spin probes, 2,2,6,6-tetramethyl-1-piperidin-*N*-oxyl and 2,2,5,5-tetramethyl-1-pyrrolidinyloxy (hereafter Tempo and Proxyl, respectively, see Figure 1) in the gas phase as well as in a polar aprotic solvent, dimethyl sulfoxide (DMSO). Nitroxide (aminoxyl) derivatives are by far the most exploited spin-label/probe molecules in ESR experiments, thanks to a long-living spin-unpaired electronic ground state and to molecular properties strongly dependent on the structure, the dynamics and the chemical environment.[18] As a matter of fact, the importance of an effective theoretical description of the effects of the chemical surroundings on nitroxide magnetic properties, including both solvent bulk properties and specific nitroxide−solvent interactions, has been pointed out in recent literature.[19,20] In particular, the differences observed among ESR spectra in various solvents have been qualitatively interpreted with reference to a selective stabilization of one of the two resonance structures depicted in Scheme 1.[21]

SCHEME 1

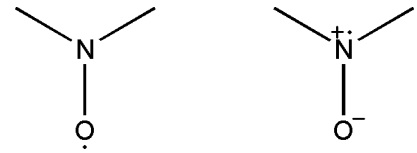

It has been demonstrated that a polar environment stabilizes the charge-separated form, with an increased spin density on the nitrogen atom. Additionally, direct specific interactions between the solvent and the NO moiety, as in the case of aqueous solution with the formation of H-bonds, may have a role comparable to that of the bulk dielectrics.[20]

Computational Details

All the calculations were performed with a local version of the Gaussian09 suite of programs.[22]

For the simulation of all structural, dynamic, and magnetic properties, we always employed the same level of theory, namely the parameter-free PBE0[23] density functional, which includes an amount of exact exchange, and the polarized double-ζ basis set N07D, purposely tailored for DFT-based calculations of magnetic parameters.[24]

Calculations of minimum energy structures were carried out using a tight criterion for both the self-consistent field and the geometry optimization convergence thresholds.[25] Solution of the vibrational Hamiltonian within the harmonic approximation was easily achieved thanks to the availability of analytical Hessian, which also allowed evaluation of semidiagonal quartic force fields through the numerical differentiation (with the standard 0.025 Å step) of analytical second derivatives. Then, anharmonicity of nuclear motions was accounted for by means of an accurate yet feasible second-order perturbation scheme.[6]

Atom-centered density matrix propagation (ADMP) MD simulations were performed in the gas phase and in DMSO solution. The time step for the numerical integration of the equations of motions was set to 0.2 fs, for a trajectory of ∼15 and ∼18 ps in the case of Proxyl and Tempo, respectively. The electron fictitious mass parameter was set to 0.5 amu $bohr^2$.

These choices of electron mass and time step were calibrated for keeping under control the adiabaticity and idempotency of the electronic density matrix along the trajectory, reasonably

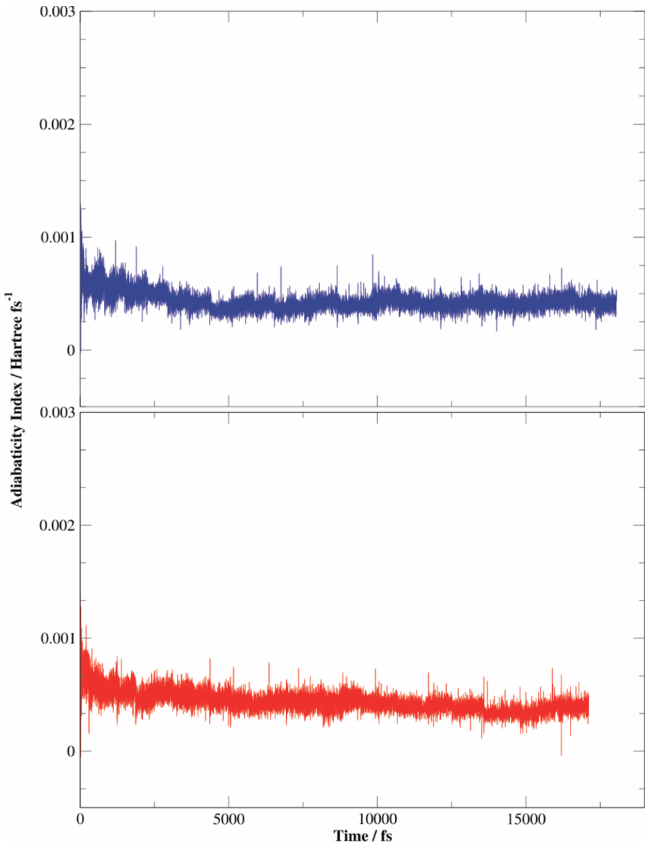

Figure 2. Evolution of the adiabaticity index along the ADMP trajectories of Tempo in the gas phase (upper panel) and DMSO trajectory (lower panel).

within the proper suggested thresholds,.[11b,e] For purposes of illustration, Figure 2 shows the behavior of the adiabaticity index for the simulations involving the Tempo radical. The translational motion and the total angular momentum were projected out at each time step, while an average temperature of 298 K was pursued via rescaling of nuclei's velocity modulus.[26]

Nonprotic polar solvents do not show a specific structuration around the solute (short residence time or high exchange rate of solvent molecules). As a consequence, both microsolvation and bulk solvent effects can be adequately accounted for, on average, by an accurate implicit model. In our experience,[4] the polarizable continuum model (PCM) can accurately describe the dipolar nature of nitroxide−DMSO interactions, and the capability of the ADMP to safely propagate the density matrix within a self-consistent reaction field has been previously demonstrated.[27,28] Therefore, AIMD simulations in DMSO solution were performed via the conductor-like polarizable continuum model (CPCM),[29] within the new continuum surface charge formalism.[30,31]

Magnetic tensors were computed on frames extracted along the trajectories each 25 fs for a total number of frames of ∼500 and of ∼600 in the case of Proxyl and Tempo, respectively; in both cases the first 3 ps of the AIMD simulations were taken out as equilibration: such sampling scheme ensures well-converged average values of magnetic parameters.[19,20]

Isotropic hyperfine coupling constants (hcc's) are proportional to electron spin densities ρ_s at or near the position of the corresponding magnetic nuclei. In the present work, we will only consider the isotropic Fermi contact term at the nitrogen nucleus, which is given by

$$\mathrm{hcc_N} = (8\pi/3) g_n g_e \mu_n \mu_e \rho_s(r_N) \quad (1)$$

where μ_n and g_n are respectively the magneton and the g factor of the nucleus, μ_e is the Bohr magneton, and g_e is the g value for the electron; finally $\rho_s(r_N)$ is the electron spin density at the nitrogen nuclear position.

For what concerns the **g** tensor, we refer to the shift from the free-electron value ($g_e = 2.002\,319$), which can be dissected into three main contributions:

$$\Delta g = \Delta g^{\mathrm{RMC}} + \Delta g^{\mathrm{GC}} + \Delta g^{\mathrm{OZ/SOC}} \quad (2)$$

Δg^{RMC} and Δg^{GC} are first-order contributions, which take into account relativistic mass (RMC) and gauge (GC) corrections, respectively. These two terms are usually small and have opposite signs so that their contributions tend to cancel out.[32]

The last term in eq 2, $\Delta g^{\mathrm{OZ/SOC}}$, is a second-order contribution arising from the coupling of the orbital Zeeman (OZ) and the spin−orbit coupling (SOC) operators. The OZ contribution shows a gauge origin dependence. In our calculations, the gauge including atomic orbital (GIAO) approach is used to solve this dependence.[33]

Finally, the SOC term involves a true two-electron operator, which will be approximated here by a one-electron operator involving adjusted effective nuclear charges. This approximation has been proven to work fairly well in the case of light atoms, providing results close to those obtained using more refined expressions for the SOC operator.[33,34] Spin-unrestricted calculations were performed providing the Kohn−Sham (KS) zero-order molecular orbitals. The magnetic field dependence was taken into account using the coupled-perturbed KS formalism, similarly as described by Neese,[34] but including the GIAO approach. Solution of the coupled perturbed KS equation (CP-KS) leads to the determination of the OZ/SOC contribution.[33]

As mentioned above, all the magnetic parameters were computed at the PBE0 level of theory employing the N07D basis set, and the CPCM when accounting for DMSO solutions; such an approach has been validated in recent systematic studies for both hyperfine[24] and **g**[35] tensors. Both in the gas phase and in liquid solutions, the radical motions are fast enough to lead to complete rotational averaging, so that the quantity directly related to experiments is actually the isotropic shift, $\Delta g_{\mathrm{iso}} = (1/3)\mathrm{Tr}(\mathbf{g} - g_e)$, and we consider in the following only this value.

Results and Discussion

The most relevant structural parameters of the minimum-energy geometry and their average along AIMD trajectories for the proxyl and tempo in the gas phase are listed in Table 1.

The main structural differences between these two radicals are due to the ring backbone: in the case of Proxyl, the five-atom ring leads to a planar conformation of the NO moiety (the oxygen atom lies in the plane defined by $C_\alpha-N-C_\alpha$) and to a projection of the oxygen atom out of the crowded space of methyl groups ($C_\alpha-N-C_\alpha$ angle of 115°); in the second case, the six-atom ring leads to a nonplanar nitroxide moiety ($C_\alpha-N-O\cdots C_\alpha$ improper dihedral angle close to 20°), and also the backbone $C_\alpha-N-C_\alpha$ angle of 124° corresponds to an oxygen atom less exposed to the external space. Additionally, the different NO bond length values can be rationalized by the overall nitroxide backbones. In the planar NO moiety of Proxyl, both N and O atoms show a nominal sp^2 hybridization, whereas in the nonplanar case of Tempo, the N hybridization is close to sp^3, leading to an elongation of the NO equilibrium bond length.

TABLE 1: Structural and Magnetic Parameters of Proxyl and Tempo in the Gas Phase Obtained from Minimum-Energy Geometry or Averaged along AIMD Trajectories[a]

gas phase	$Proxyl_{OPT}$	$\langle Proxyl\rangle_{AIMD}$	$Tempo_{OPT}$	$\langle Tempo\rangle_{AIMD}$
N−O bond	1.260	1.26 (0.02)	1.269	1.27 (0.02)
C_α−N−C_α angle	115.3	115 (3)	124.3	124 (4)
C_αNO···C_α dihedral	0.0	0 (16)	21.4	0 (20)
|C_αNO···C_α|	0.0	12 (10)	21.4	16 (10)
hcc_N	11.8	14 (2)	14.8	15 (3)
Δg_{iso}	3338.1	3361 (193)	3637.0	3591 (250)

[a] Distances in Å, valence and dihedral angles in degrees, hcc_N in gauss, and Δg_{iso} in ppm; standard deviations are given in parentheses.

TABLE 2: Isotropic Nitrogen Hyperfine Coupling Constant (hcc_N) (in gauss), Computed on Minimum-Energy Geometries Including Quantum Vibrational Effects (at 298 K), and Harmonic, Anharmonic, and Total Vibrational Contributions (Δhcc_N)

	$\langle Proxyl\rangle_{Harm}$	$\langle Proxyl\rangle_{Anharm}$	$\langle Proxyl\rangle_{Tot}$	expt[a]
hcc_N	11.9	14.3	14.4	14.02
Δhcc_N	0.1	2.5	2.6	
	$\langle Tempo\rangle_{Harm}$	$\langle Tempo\rangle_{Anharm}$	$\langle Tempo\rangle_{Tot}$	expt[b]
hcc_N	14.2	15.2	14.6	15.28
Δhcc_N	−0.6	0.4	−0.2	

[a] Value in dodecane solution, ref 19. [b] Value in cyclohexane solution, ref 20.

Values averaged over AIMD trajectories mostly confirm their minimum-energy counterparts, the most significant discrepancy between "static" and "dynamic" pictures regarding the out-of-plane bending of the NO moiety, which gives rise, according to standard deviations, to large-amplitude motions. For both radicals the average configuration is planar, but the average over absolute values of the C_α−N−O···C_α improper dihedral angle changes the picture leading to a pyramidal most probable structure for both nitroxides. In essence, the out-of-plane angle oscillates between positive and negative values, which are equivalent for the pseudosymmetric plane of the NO moiety.

Table 1 also reports the hcc_N and Δg_{iso} values of the minimum-energy structures and the ones averaged over the AIMD trajectories. We recall that the isotropic hyperfine coupling is a local quantity (i.e., a direct measure of the coupling between the spin-unpaired electron and the magnetic moment of a specific nucleus), whereas the isotropic **g**-tensor shift accounts for the total electronic structure of the paramagnetic molecules.[4] Comparison of hcc_N values computed on the optimized geometries and along AIMD trajectories presents the same behavior as for the structural parameters: vibrational effects are relevant in the case of Proxyl, with a shift of ∼2 G, whereas they are negligible in the case of Tempo. Indeed, the significant standard deviations in both the Proxyl and Tempo cases are related to a high flexibility of the molecules on one hand, and to the short statistics of AIMD simulations on the other.

However, as listed in Table 2 for both radicals, comparison to hcc_N computed accounting the QM vibrational averaging by our time-independent approach[4] confirms fully the AIMD results. The availability of normal modes and of the derivatives of the observables with respect to them allowed us to evaluate the contributions of different vibrations to the overall hcc_N values. In the case of Proxyl, the total vibrational effect on the hcc_N amounts to 2.6 G: the anharmonic correction is crucial because it is responsible for 96% of the total shift from the equilibrium structure. Additionally, just three normal modes are responsible for 84% of the total effect, namely the C_α−N−O···C_α improper dihedral bending (43% of the total shift), N−O out-of-plane bending (31%) and the C_α−N−C_α out-of-plane bending (10%): all these modes are related to inversion at the nitrogen atom. The overall contribution of all the other vibrations amounts to 0.41 G, none of them participating to the total correction by more than 3%. In the case of Tempo, the total vibrational effects are negligible (−0.2 G) due to comparable harmonic and anharmonic contributions which have, however, an opposite sign (−0.57 and 0.37 G, respectively). As a consequence, equilibrium and vibrationally averaged hcc_N values are very close.

It is noteworthy that the hcc_N values issuing from AIMD averaging and from time-independent QM perturbative treatment are in quantitative agreement with each other and with experimental hcc_N values observed in apolar and aprotic solvents characterized by very low dielectric constants.[36,37] Thereafter, it appears clearly that in the case of Proxyl considering only the minimum-energy hcc_N value or only the harmonic approximation leads to results that are qualitatively unreliable and quantitatively far from their experimental counterparts. In the case of Tempo, the final agreement between static minimum-energy values and the ones where dynamics is properly taken into account through AIMD average or anharmonic calculations is caused by a fortuitous cancellation of effects. Nevertheless, this does not mean that neglecting the molecular dynamics represents a safe and reliable computational strategy.

The remarkable quantitative agreement among the perturbative anharmonic, AIMD averaged, and experimental values recorded in very low dielectric solvents provides us a safe ground for a confident analysis of the qualitative effects of MD in tuning the magnetic properties of spin probe nitroxides. In particular, by plotting the hcc_N values with respect to the out-of-plane angle of the NO moiety along the Proxyl and Tempo trajectories (Figure 3), we can settle some further insight. For both radicals, an almost parabolic relationship can be observed, with the hcc_N value increasing when going from a planar to a pyramidal nitroxide conformation. However, while the planar structure is the minimum-energy configuration for Proxyl, in the case of Tempo it corresponds to a transition state governing inversion between two equivalent pyramidal energy minima. The trends observed for hcc_N can be put into a more general perspective[4] by remembering that both direct and spin-polarization contributions to hcc_N are roughly proportional to the spin population in the singly occupied highest energy molecular orbital (SOMO). In the planar conformation (which we have seen does not necessarily correspond to a minimum on the PES), the only contribution to the hcc_N is related to spin polarization; however, pyramidalization at the nitrogen center allows for the direct involvement of the nitrogen s-type orbital in the SOMO (as qualitatively depicted for Proxyl in Figure 4), leading to a large direct contribution to the Fermi contact term, which overcomes the spin-polarization one and determines the observed increase.

Coming next to the **g**-tensor shift, we recall that a qualitative explanation of its behavior in organic free radicals is provided by the Stone theory.[38,39] In these systems, the significant amount of spin density localized on heteroatoms such as nitrogen or oxygen leads to a distinct **g**-tensor anisotropy. This is related on the one hand to the relatively large spin−orbit coupling constants of heteroatoms, which results in significant spin−orbit mixing and, on the other hand, to the presence of nonbonding orbitals that are energetically close to the SOMO. In the specific case of nitroxide radicals, the most relevant contribution to this term comes from an electronic excitation from the SOMO-1

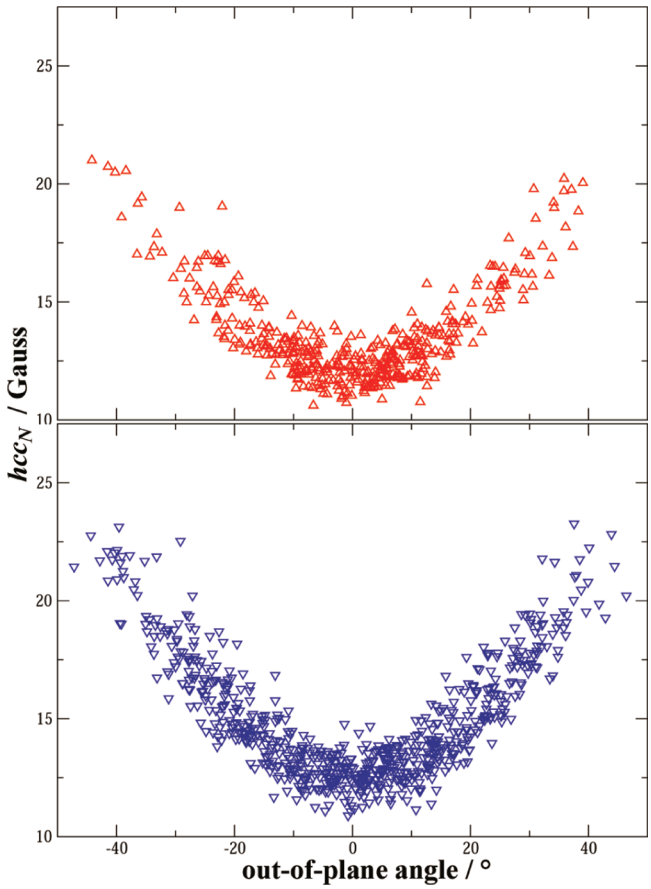

Figure 3. Correlation plots between hcc_N and nitroxide out-of-plane angle (corresponding to the $C_\alpha-N-O\cdots C_\alpha$ improper dihedral angle) as computed along AIMD trajectories; upper panel, Proxyl; lower panel, Tempo.

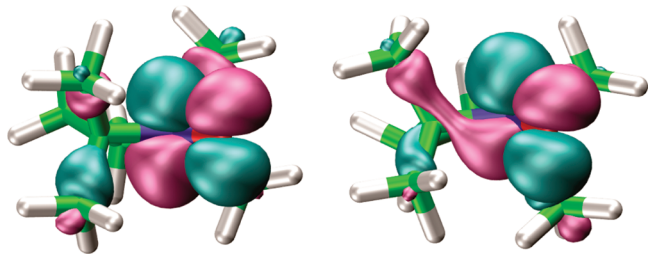

Figure 4. Isodensity surface of Proxyl's SOMO from a planar configuration (left) to a pyramidal one (right).

(an in-plane lone pair, hereafter referred to as n) to the SOMO (an out-of-plane π^* orbital).[40,41] The effects of molecular dynamics on the isotropic g-shift term are very weak (about 1% of the total shift), whereas the influence of the solvent dielectrics is more relevant. The latter effect is related to the selective stabilization of lone pair orbitals by polar solvents; this increases the $n-\pi^*$ gap, with the consequent reduction of **g**-tensor shifts. Also, the slight lengthening of the NO bond when going from gas phase to DMSO solution has a negligible effect on lone pair orbitals, but stabilizes the π^*-SOMO; this results in a smaller $n-\pi^*$ gap and to larger **g**-tensor values, but nevertheless this effect has a lower impact than the direct electrostatic effects of the solvent. The effects of the DMSO solvent on the molecular structures and magnetic parameters are listed in Table 3: the shift of Δg_{iso} from gas phase to DMSO goes in the same direction for both the nitroxide probes, but the relative variations are smaller than those due to structural changes and vibrational averaging, being around 5% of the total shift in DMSO.

TABLE 3: Structural and Magnetic Parameters of Proxyl and Tempo in DMSO from Minimum-Energy Geometry and Averaged along AIMD Trajectories[a]

DMSO solution	$Proxyl_{OPT}$	$\langle Proxyl\rangle_{AIMD}$	$Tempo_{OPT}$	$\langle Tempo\rangle_{AIMD}$
N−O bond	1.264	1.27 (0.02)	1.271	1.27 (0.02)
$C_\alpha-N-C_\alpha$ angle	115.2	115 (3)	124.4	124 (4)
$C_\alpha NO\cdots C_\alpha$ dihedral	0.0	0 (18)	19.9	0 (17)
$\lvert C_\alpha NO\cdots C_\alpha\rvert$	0.0	16 (9)	19.9	15 (10)
hcc_N	13.0	15 (2)	15.4	15 (2)
Δg_{iso}	3186.2	3255 (178)	3477.3	3432 (225)

[a] Distances in Å, valence and dihedral angles in degrees, hcc_N in gauss, and Δg_{iso} in ppm; standard deviations are given in parentheses.

Concerning the hcc_N shift, when going from gas phase to solution, we obtained results in qualitative agreement with the experimental observations regarding a similar nitroxide (∼1 G).[21] Besides the quantitative comparison with experiments, we would like to stress that computational studies allow to assess the decoupling of molecular dynamics and solvent effects on the final value of the molecular parameter. It appears from our results that dynamical effects are not affected by the presence of the solvent; i.e., the hcc_N shifts from the minimum-energy structure (optimized in the presence of the solvent) with respect to the average along the AIMD are ∼2 G in the case of Proxyl and smaller than 1 G for Tempo. So, a consistent solvent shift is predicted for both equilibrium properties or the ones obtained by averaging over AIMD trajectories.

Conclusions

The present contribution reports the accurate prediction of ESR parameters for two very widely used spin probes, namely the Proxyl and Tempo nitroxide radicals. Beyond the mere reproduction of experimental results, we addressed the roles that molecular dynamics and aprotic polar solvents (here DMSO) play in tuning the magnetic properties. Furthermore, from a methodological point of view, we tested the effectiveness of time-dependent and time-independent routes for an accurate modeling of these subtle effects. It has been shown that both approaches allow a proper vis-a-vis comparison of experimental and theoretical results, as well as an effective evaluation and dissection of dynamical effects determining spectral properties. Additionally, we demonstrated that classical MD can be safely employed for accounting for vibrational effects, at the condition that ab initio or semiempirical force fields are purposely tuned for both the system of interest and the targeted molecular property.

Our results highlight that accounting for thermal fluctuations is of paramount importance for state-of-the-art molecular modeling of sensitive molecular properties like spectroscopic parameters. In particular, in the case of isotropic hyperfine coupling constants, which are among the most exploited ESR observables, neglecting nuclear motions could lead to qualitatively misleading results.

References and Notes

(1) Barone, V.; Improta, R.; Rega, N. *Acc. Chem. Res.* **2008**, *41*, 605.
(2) Zerbetto, M.; Polimeno, A.; Barone, V. *Comput. Phys. Commun.* **2009**, *180*, 2680.
(3) (a) Barone, V.; Bloino, J.; Biczysko, M.; Santoro, F. *J. Chem. Theory. Comput.* **2009**, *5*, 540. (b) Santoro, F.; Barone, V. *Int. J. Quantum Chem.* **2010**, *110*, 476.
(4) Improta, R.; Barone, V. *Chem. Rev.* **2004**, *104*, 1231.
(5) Wilson, E. B.; Decious, J. C.; Cross, P. C. *Molecular Vibrations*; McGraw Hill: New York, 1955.

(6) Barone, V. *J. Chem. Phys.* **2005**, *122*, 014108.

(7) Barone, V.; Biczysko, M.; Cimino, P. Interplay of Stereoelectronic Vibrational and Environmental Effects in Tuning Physicochemical Properties of Carbon-Centered Radicals. In *Carbon-Centered Free Radicals and Radical Cations*; Forbes, M. D. E., Ed.; John Wiley & Sons: New York, 2010; p 105.

(8) (a) Leach, A. R. *Molecular Modeling: Principles and Applications*; Pearson Education: Harlow, UK, 2001. (b) Cimino, P.; Pedone, A.; Stendardo, E.; Barone, V. *Phys. Chem. Chem. Phys.* **2010**, *12*, 3741.

(9) (a) Car, R.; Parrinello, M. *Phys. Rev. Lett.* **1985**, *55*, 2471. (b) Marx, D.; Hutter, J. *Ab Initio Molecular Dynamics: Basic Theory and Advanced Methods*; Cambridge University Press: Cambridge, UK, 2009.

(10) Parr., R. G.; Yang, W. *Density-Functional Theory of Atoms and Molecules*; Oxford University Press: New York, 1989.

(11) (a) Schlegel, H. B.; Millam, J. M.; Iyengar, S. S.; Voth, G. A.; Daniels, A. D.; Scuseria, G. E.; Frisch, M. J. *J. Chem. Phys.* **2001**, *114*, 9758. (b) Iyengar, S. S.; Schlegel, H. B.; Millam, J. M.; Voth, G. A.; Scuseria, G. E.; Frisch, M. J. *J. Chem. Phys.* **2001**, *115*, 10291. (c) Schlegel, H. B.; Iyengar, S. S.; Li, X. S.; Millam, J. M.; Voth, G. A.; Scuseria, G. E.; Frisch, M. J. *J. Chem. Phys.* **2002**, *117*, 8694. (d) Rega, N.; Iyengar, S. S.; Voth, G. A.; Schlegel, H. B.; Vreven, T.; Frisch, M. J. *J. Phys. Chem. B* **2004**, *108*, 4210. (e) Iyengar, S. S.; Schlegel, H. B.; Voth, G. A.; Millam, J. M.; Scuseria, G. E.; Frisch, M. J. *Isr. J. Chem* **2002**, *7*, 191.

(12) (a) Barone, V.; Biczysko, M.; Brancato, G. Extending the Range of Computational Spectroscopy by QM/MM Approaches. Time-dependent and Time-independent routes. In *Combining Quantum Mechanics and Molecular Mechanics. Some Recent Progresses in QM/MM*; Sabin, J., Canuto, S., Eds.; Advances in Quantum Chemistry Vol. *59*; Academic Press: New York, 2010; p 17. (b) Iyengar, S. S. *J. Chem. Phys.* **2005**, *123*, 084310. (c) Iyengar, S. S.; Petersen, M. K.; Burnham, C. J.; Day, T. J. F.; Teige, V. E.; Voth, G. A. *J. Chem. Phys.* **2005**, *123*, 084309. (d) Iyengar, S. S. *J. Chem. Phys.* **2007**, *126*, 216101. (e) Li, X.; Teige, V. E.; Iyengar, S. S. *J. Phys. Chem. A* **2007**, *111*, 4815–4820. (f) Li, X.; Moore, D. T.; Iyengar, S. S. *J. Chem. Phys.* **2008**, *128*, 184308.

(13) (a) Bernasconi, L.; Sprik, M.; Hutter, J. *J. Chem. Phys.* **2003**, *119*, 12417. (b) Sulpizi, M.; Carloni, P.; Hutter, J.; Röthlisberger, U. *Phys. Chem. Chem. Phys.* **2003**, *5*, 4798. (c) Crescenzi, O.; Pavone, M.; De Angelis, F.; Barone, V. *J. Phys. Chem. B* **2005**, *109*, 445.

(14) (a) Röhrig, U. F.; Frank, I.; Hutter, J.; Laio, A.; VandeVondele, J.; Röthlisberger, U. *ChemPhysChem* **2003**, *4*, 1177. (b) Mercier, S. R.; Boyarkin, O. V.; Kamariotis, A.; Guglielmi, M.; Tavernelli, I.; Cascella, M.; Rothlisberger, U.; Rizzo, T. R. *J. Am. Chem. Soc.* **2006**, *128*, 16938.

(15) (a) Sebastiani, D.; Parrinello, M. *ChemPhysChem* **2002**, *3*, 675. (b) Komin, S.; Gossens, C.; Rothlisberger, U.; Sebastiani, D. *J. Phys. Chem. B* **2007**, *111*, 5225. (c) Grigoleit, S.; Bühl, M. *J. Chem. Theory Comput.* **2005**, *1*, 181. (d) Pavone, M.; Barone, V.; Ciofini, I.; Adamo, C. *J. Chem. Phys.* **2004**, *120*, 9167.

(16) (a) Asher, J. R.; Kaupp, M. *Theor. Chem. Acc.* **2008**, *119*, 477. (b) Asher, J. R.; Doltsinis, N. L.; Kaupp, M. *J. Am. Chem. Soc.* **2004**, *126*, 9854.

(17) (a) Schneider, D. J.; Freed, J. H. *Adv. Chem. Phys.* **1989**, *73*, 387. (b) Barone, V. A.; Polimeno, A. *Phys. Chem. Chem. Phys.* **2006**, *8*, 4609.

(18) (a) Berliner, L. J. *Spin Labelling, Theory and Applications*; Academic Press: New York, 1976. (b) Mattar, S. M.; Sanford, J. *J. Phys. Chem. A* **2009**, *113*, 11435.

(19) Pavone, M.; Cimino, P.; De Angelis, F.; Barone *J. Am. Chem. Soc.* **2006**, *128*, 4338.

(20) (a) Pavone, M.; Cimino, P.; Crescenzi, O.; Sillanpaa, A.; Barone, V. *J. Phys. Chem. B* **2007**, *111*, 8928. (b) Pavone, M.; Sillanpaa, A.; Cimino, P.; Crescenzi, O.; Barone, V. *J. Phys. Chem. B* **2006**, *110*, 16189. (c) Pavone, M.; Benzi, C.; De Angelis, F.; Barone, V. *Chem. Phys. Lett.* **2004**, *395*, 120.

(21) Knauer, B. R.; Napier, J. J. *J. Am. Chem. Soc.* **1976**, *91*, 4395.

(22) *Gaussian 09, Revision A02*; Frisch, M. J.; Trucks, G. W.; Schlegel, H. B.; Scuseria, G. E.; Robb, M. A.; Cheeseman, J. R.; Scalmani, G.; Barone, V.; Mennucci, B.; Petersson, G. A.; Nakatsuji, H.; Caricato, M.; Li, X.; Hratchian, H. P.; Izmaylov, A. F.; Bloino, J.; Zheng, G.; Sonnenberg, J. L.; Hada, M.; Ehara, M.; Toyota, K.; Fukuda, R.; Hasegawa, J.; Ishida, M.; Nakajima, T.; Honda, Y.; Kitao, O.; Nakai, H.; Vreven, T.; Montgomery, Jr., J. A.; Peralta, J. E.; Ogliaro, F.; Bearpark, M.; Heyd, J. J.; Brothers, E.; Kudin, K. N.; Staroverov, V. N.; Kobayashi, R.; Normand, J.; Raghavachari, K.; Rendell, A.; Burant, J. C.; Iyengar, S. S., Tomasi, J., Cossi, M.; Rega, N.; Millam, N. J.; Klene, M.; Knox, J. E.; Cross, J. B.; Bakken, V.; Adamo, C.; Jaramillo, J.; Gomperts, R. E.; Stratmann, O.; Yazyev, A. J.; Austin, R.; Cammi, C.; Pomelli, J. W.; Ochterski, R.; Martin, R. L.; Morokuma, K.; Zakrzewski, V. G.; Voth, G. A.; Salvador, P.; Dannenberg, J. J.; Dapprich, S.; Daniels, A. D.; Farkas, O.; Foresman, J. B.; Ortiz, J. V.; Cioslowski, J.; Fox, D. J. Gaussian, Inc.: Wallingford, CT, 2009.

(23) Adamo, C.; Barone, V. *J. Chem. Phys.* **1999**, *110*, 6158.

(24) (a) Barone, V.; Cimino, P. *Chem. Phys. Lett.* **2008**, *454*, 139. (b) Barone, V.; Cimino, P. *J. Chem. Theory Comput.* **2009**, *5*, 192.

(25) Foresman, J. B.; Frish, A. E. *Exploring Chemistry With Electronic Structure Methods*; Gaussian Inc.: Wallingford, CT, 1996.

(26) Allen, M. P.; Tidsley, D. J. *Computer Simulation of Liquids*; Clarendon Press: Oxford, UK, 1987.

(27) Rega, N. *Theor. Chem. Acc.* **2006**, *116*, 347.

(28) Brancato, G.; Rega, N.; Barone, V. *J. Chem. Phys.* **2006**, *124*, 214505.

(29) Cossi, M.; Rega, N.; Scalmani, G.; Barone, V. *J. Comput. Chem.* **2003**, *24*, 669.

(30) York, D. M.; Karplus, M. *J. Phys. Chem. A* **1999**, *103*, 11060.

(31) Scalmani, G.; Frisch, M. J. Private communication.

(32) Stone, A. J. *Proc. R. Soc. London, Ser. A* **1963**, *271*, 424.

(33) (a) Cheesman, J. R.; Trucks, G. W.; Keith, T. A.; Frisch, M. J. *J. Chem. Phys.* **1998**, *104*, 5497. (b) Ditchfield, R. *Mol. Phys.* **1974**, *27*, 789. (c) Malkina, O. L.; Vaara, J.; Schimmelpfenning, B.; Munzarova, M. L.; Malkin, V. G.; Kaupp, M. *J. Am. Chem. Soc.* **2000**, *122*, 9206.

(34) Neese, F. *J. Chem. Phys.* **2001**, *115*, 11080.

(35) Barone, V.; Cimino, P. *J. Chem. Theory. Comput.* **2009**, *5*, 192.

(36) Keana, J. F. W.; Lee, T. D.; Bernard, E. M. *J. Am. Chem. Soc.* **1976**, *98*, 3052.

(37) Franchi, P.; Lucarini, M.; Pedrielli, P.; Pedulli, G. F. *ChemPhysChem* **2002**, *3*, 789.

(38) Stone, A. J. *Mol. Phys.* **1963**, *6*, 509.

(39) Stone, A. J. *Mol. Phys.* **1964**, *7*, 311.

(40) Rinkevicius, Z.; Telyatnyk, L.; Vahtras, O.; Ruud, K. *J. Chem. Phys.* **2004**, *121*, 5051.

(41) Sinnecker, S.; Rajendran, A.; Klamt, A.; Diedenhofen, M.; Neese, F. *J. Phys. Chem. A* **2006**, *110*, 2235.

JP102232C